Interaction of mutant p53 with p73: A Surface Plasmon Resonance and Atomic Force Spectroscopy study

CrossMark

Simona Santini [a], Silvia Di Agostino [b], Emilia Coppari [a], Anna Rita Bizzarri [a], Giovanni Blandino [b], Salvatore Cannistraro [a,*]

[a] Biophysics and Nanoscience Centre, CNISM, Dipartimento DEB, Università della Tuscia, Viterbo, Italy
[b] Translational Oncogenomic Unit, Italian National Cancer Institute 'Regina Elena'-IFO, via Elio Chianesi 53, 00144 Rome, Italy

ARTICLE INFO

ABSTRACT

Background: TP53 tumor suppressor gene is mutated in more than 50% of human tumors. Mutated p53 proteins could sequestrate and inactivate p73 reducing the apoptotic and anti-proliferative effects of the transcription factor, and yielding cancer cells more aggressive and chemoresistant. The possibility of using drugs to prevent the mutant p53/p73 complex formation preserving the p73 function, calls for a deeper insight into the molecular and biochemical mechanisms of mutant p53/p73 protein interaction.
Methods: The kinetics of the mutant p53R175H/p73 complex was investigated with innovative and complementary techniques, operating in real time, in near physiological conditions and without any labeling. Specifically, Atomic Force Spectroscopy and Surface Plasmon Resonance working at single-molecule level and in bulk condition, respectively, were used.
Results: The two techniques revealed that a stable complex is formed between mutant p53R175H and p73 proteins; the complex being characterized by a high interaction force and a dissociation equilibrium constant in the order of 10^{-7} M, as expected for specific interactions. No binding was instead observed between p73 and wild type p53.
Conclusions: Mutant p53R175H protein, unlike wild type p53, can form a stable complex with p73. The mutant p53R175H/p73 protein complex could be a target for innovative pharmaceutical drugs that, by dissociating it or preventing biomolecule interaction thus preserving the p73 function, could enhance the response of cancerous cells carrying mutant p53R175H protein to common chemotherapeutic agents.
General significance: The kinetic information obtained *in vitro* may help to design specific pharmaceutical drugs directed against cancerous cells carrying mutant p53 proteins.

© 2014 Elsevier B.V. All rights reserved.

1. Introduction

p53 is a tumor suppressor protein called the "*guardian of the genome*" [1] for its crucial role in the cell cycle progression control and coordination of cellular response to a broad range of stress factors ensuring the maintenance of genomic stability and the prevention of cancer development [2–4]. Tumors expressing a mutant p53 protein (mutp53) are characterized by high genomic instability, resistance to chemotherapy and invasiveness. These new characteristics constitute the main features cancer cells acquire when the tumor suppressor p53 gene undergoes gain-of-function (GOF) mutations [4]. More than 50% of human cancers carry *TP53* mutations that abrogate its wild type function [3,5]. Although two thirds of mutations in the DNA-binding domain of p53 abolish the p53 ability to transactivate its target genes through

the p53 consensus sequences onto the promoters, the modulation of gene transcription by mutp53 is well documented as an important GOF mechanism. Probably mutp53 acts as an adaptor or mediator that links specific transcription factors to the general transcription apparatus. It has been shown how mutp53 reaches target gene promoters through the interaction with sequence-specific transcription factors, such as NF-Y, E2F1, NF-kB and the Vitamin D receptor [6–9]. In such aberrant cells, the p53 activity could be, at least in part, vicariated by two members of its family, p63 and p73, that share high structural and functional homology with p53 [10–13]. In fact, both p63 and p73 are activated by the same signaling pathways that lead to the p53 activation and stimulate the transcription of p53 responsive genes controlling cell proliferation, differentiation and death [14]. Furthermore mutp53, unlike the wild type p53 (wtp53), can interact and sequester both p73 and p63 family members, abrogating their antitumoral function [15–17]. In particular, many evidences indicate that p73 loss of function in p53 defective cells not only contributes to the insurgence, maintenance and spreading of human cancers [18–20], but it is also a major determinant of human tumor chemoresistance [21–23]. In this context, the efforts to

search innovative pharmaceutical drugs and molecules able to dissociate the aberrant mutp53/p73 protein complex [24] safeguarding the p73 activity are arousing greater interest. Of course, a deeper knowledge of the molecular and biochemical interaction mechanisms underlying the formation of the mutp53/p73 complex, could help to design more specific drugs. In particular, the present work is aimed at shedding light on the kinetics of the interaction between full length p73 and the conformational mutant p53R175H (mutp53R175H) proteins, the latter having a point mutation of codon 175 of the *TP*53 gene. Such an interaction has been already detected both *in vitro* and *in vivo* [15,16,24]. Indeed, it is believed that this interaction severely impairs the p73-mediated transcriptional activity and apoptosis in response to anticancer drugs by sequestering p73 away from its target gene promoters [16,24]. These evidences emerge in human large lung carcinoma and breast cancer cells where p53 is mutated [16,24]. The mutp53R175H/p73 protein interaction has been studied here using two innovative and complementary techniques, Atomic Force Spectroscopy (AFS) and Surface Plasmon Resonance (SPR). AFS is a nanotechnological-based approach able to detect piconewton interaction forces between a tip-anchored molecule and its substrate-immobilized partner, even at single molecule level, in near native conditions and without any label or sample preparation [25,26]. On the other hand, SPR is a flexible and powerful approach providing the kinetic and equilibrium characterization of binding processes occurring between a sensor chip immobilized ligand and its partner free in solution [27,28]. Taken together, the AFS and SPR results demonstrate that mutp53R175H protein forms a high affinity complex with p73. At single molecule level, such a complex is characterized by a dissociation rate constant typical of specific complexes, as well by a high interaction force and a single barrier in the energy landscape. No interaction has been instead monitored between p73 and wild type p53.

2. Material and methods

2.1. GST-protein expression and purification

Escherichia coli cells (BL21DE3) transformed with pGEX-4X-mutp53R175H, pGEX-4X-wtp53 and pGEX-4X-p73 vectors were grown at 37 °C in LB medium containing 100 μg/ml ampicillin to an optical density at 600 nm of 0.4. The expression of recombinant proteins was induced by the addition of 0.5 mM isopropyl-1-thio-β-galactopyranoside (IPTG) for 3 h at the same temperature under vigorous shaking. Bacteria were pelleted and lysed in phosphate-buffered saline (PBS 1×) containing 0.1% Triton X-100, 1 mM DTT, and protease inhibitors, by probe sonication (three cycles of 1 min each). The sonicate was clarified by centrifugation at 13.000 rpm and supernatant fractions were incubated with glutathione-Sepharose beads (Sigma, G 4510) for 1 h at 4 °C with constant shaking. After several washes in PBS, the GST-protein beads were re-suspended in 1× PBS containing 300 mM CaCl$_2$ and 10 units of thrombin protease (Amersham Biosciences). After incubation at room temperature (RT) for 16 h, the GST-free supernatant fractions containing wtp53, mutp53R175H and p73 purified proteins were passed three times through a column containing 1 ml of *p*-aminobenzamidine-agarose beads (Sigma, A-7155). The eluates containing the purified proteins were dialyzed against storage buffer (50 mM Tris–HCl pH 7.5, 1 mM MgCl$_2$, 0.5 mM DTT). The levels of expressed proteins were checked by SDS-PAGE and Coomassie Brilliant Blue R-250 staining, while known amounts of bovine serum albumin were used as standard. Additional protein concentrations were determined by colorimetric assay (Bio-Rad, Hercules, CA, USA).

2.2. Functionalization of AFS substrate and tips

Silicon nitride Atomic Force Microscopy (AFM) tips (Veeco Instruments, Santa Barbara, CA) and glass substrates were amino-functionalized using a gas-phase method with (3-aminopropyl) triethoxysilane (APTES, Sigma) [29].

Full length p73 tumor suppressor proteins were immobilized on cover glass (Ø 12 mm). The glass was cleaned for 5 min in acetone and then irradiated by a UV lamp for 30 min to expose hydroxyl groups. The clean glass substrate was then placed at RT inside a desiccator together with the lids of two eppendorf vials in which 30 μl of APTES and 10 μl of triethylamine were separately added. The desiccator was flooded with N$_2$ to remove air and moisture. After 2 h incubation time lids were removed, the desiccator was re-flooded with N$_2$ and the substrate was left here for 2 days to cure APTES layer. Then, the glass was incubated with a solution of 1% glutaraldehyde in Milli-Q water for 3 min at RT, successively rinsed carefully with Milli-Q water and dried with nitrogen. Finally it was incubated overnight at 4 °C with a 4 μM full length p73 protein solution in Tris–HCl pH 7.4, 4% glycerol. Afterwards the substrate was gently washed with buffer to remove the unbound proteins and unreacted aldehyde groups were capped with 10 M ethanolamine-HCl 20 min incubation. Substrate was then washed again and stored at 4 °C. A scheme of the substrate preparation procedure is shown in Fig. 1A.

A very similar procedure was used to anchor full length mutp53R175H (or wtp53) protein to the AFS tip cantilever. Once the APTES layer was obtained with the gas-phase method, tips were incubated in 1% glutaraldehyde in Milli-Q water for 4 min, rinsed with Milli-Q water, dried with nitrogen and then incubated overnight at 4 °C with 4 μM mutp53R175H (or wtp53) protein. Once the tips were washed and reactive aldehyde groups quenched with ethanolamine, they were stored at 4 °C. A schematic representation of tip functionalization is shown in Fig. 1B.

2.3. Force spectroscopy measurements and unbinding detection

Force–distance curves were acquired at RT using a commercial AFM (Nanoscope IIIa/Multimode AFM Digital Instruments, Santa Barbara, CA). AFS measurements were carried out in PBS buffer (50 mM K$_3$PO$_4$, 150 mM NaCl, pH 7.5) using force calibration mode AFM. Force plots were acquired using rectangular-shaped Si$_3$N$_4$ cantilevers (Veeco probes MSNL-10) with a nominal spring constant, k_{nom}, of 0.02 N/m functionalized as described in Section 2.2. The effective spring constant of the functionalized tips, k_{eff}, was determined by following the procedure in ref. [30].

A scheme of the approach-retraction (AR) cycle performed to acquire force–distance curves is shown in Fig. 2. Starting with the tip away from the substrate and setting a ramp size of 150 nm, mutp53R175H (or wtp53) protein-functionalized tip is approached at a speed, v, of 50 nm/s to the p73 protein functionalized surface (point 1 of Fig. 2). From the contact point on (point 2), the cantilever begins to deflect due to the repulsive forces from the overlapping molecular orbitals between the tip and the substrate. The approaching phase (dotted line) keeping on, the cantilever exerts an increasing pushing force on the substrate and its deflection increases while ligand and receptor, brought in close proximity, could interact. When the cantilever exerts a force of 0.5 nN on the substrate, the approach phase is stopped to limit the maximum contact force (point 3). After 100 ms encounter time, the tip is retracted from the substrate (continuous line) at a speed ranging from 50 to 4200 nm/s, and attractive, adhesion or interaction forces formed during the contact phase, cause a downward curvature of the tip at the contact point (point 4). As far as the retraction phase continues, when the retraction force overcomes the strength of interaction between the partners, the cantilever jumps off returning to the baseline after complex dissociation (point 5). The complex unbinding force can be now determined from the product of the cantilever deflection, d, at the jump-off, by the cantilever effective spring constant, k_{eff} ($F = k_{eff} \cdot d$); the calculated unbinding force depending on the rate at which the force is applied ($r = dF / dt$), denoted loading rate, and it is given by the relationship $r = k \cdot v$, in which v is the retraction
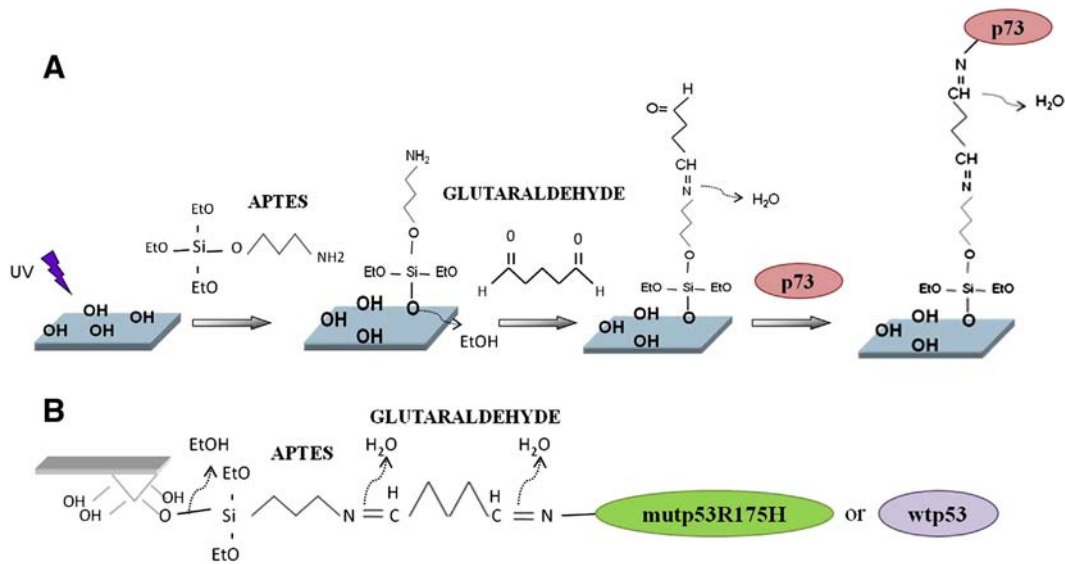
Fig. 1. Immobilization strategies of p73 and mutp53R175H (or wtp53) on the glass substrate and the AFM tip, respectively. (A) p73 protein is immobilized on glass slides via a chemical platform involving sequentially linked amino-silane and glutaraldehyde. (B) mutp53R175H or wtp53 proteins are anchored to the AFS silanized tip through the NH2 groups of lysine residues exposed on the protein surface after tip incubation with glutaraldehyde.

speed of the cantilever from the substrate [31]. The AFS experiments were thus performed at five different loading rates in the range 1–84 nN/s. Thousands of force curves were acquired at each loading rate, required to perform a statistical analysis and to obtain a reliable quantitative information from the experiments. To this aim, force curves corresponding to specific unbinding events were selected. Specifically, force curves whose retraction portion before the jump-off exhibited a non-linear trend starting and ending at the zero-deflection line, and curves presenting multiple jumps – due to subsequent rupture of the complex bonds – showing a last jump starting and ending at zero deflection, were used for the successive statistical analysis [26]. At each loading rate, the unbinding force histogram was extracted and the most probable unbinding force (F^*) was taken from the maximum of the main peak of the corresponding histogram. Thereby, the kinetic and thermodynamic parameters at the equilibrium were obtained from these non-equilibrium measurements [32], in the framework of the Bell–Evans model [31,33] which assumes a linear relationship between the most probable unbinding force, F^*, and the natural logarithm of the loading rate, r, by Eq. (1):

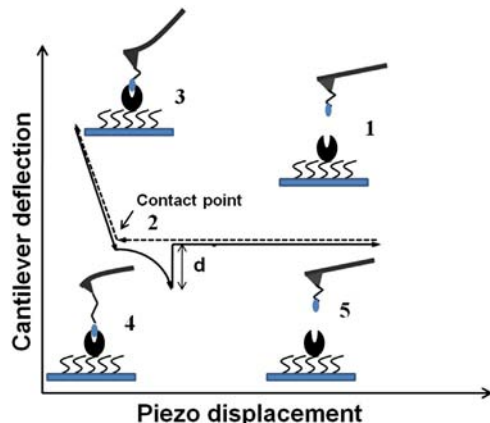$$F^* = \frac{k_B T}{x_\beta} \ln\left[\frac{r x_\beta}{(k_d k_B T)}\right] \qquad (1)$$

Fig. 2. Sketch of AFS experiments. See the text for a detailed description.

where k_B is Boltzmann's constant and T is the absolute temperature, k_d is the equilibrium dissociation rate constant, and x_β is the width of the energy barrier along the direction of the applied force. The effective loading rate r was here determined by the product between the retraction velocity and the spring constant of the entire system, k_{syst}, to take into account the contribution from molecules (i.e. proteins and/or linkers) tied to the AFM tip. The k_{syst} was thus evaluated as in Friedsam et al., 2003 [34]. Therefore, the kinetic parameters k_d and x_β were obtained from the slope and intercept of a linear fit by Eq. (1) of the plot of F^* versus ln (r).

2.4. SPR substrate preparation

SPR analysis was performed at 25 °C with a Biacore X100 system (GE Healthcare, Bio-Sciences AB, Sweden). Using a standard amine coupling chemistry [35], p73 protein (ligand) was coupled on a CM5 sensor chip surface (Fig. 3). Briefly, the carboxymethylated dextran surface of a CM5 sensor chip was first activated by a 7 min injection of a 1:1 mixture of 0.4 M N-ethyl-N-(3-diethylaminopropyl) carbodiimide (EDC) and 0.1 M N-hydroxyl-succinimide (NHS) at 10 μl/min to give reactive succinimide esters. Then a 0.02 μg/μl ligand solution in 10 mM acetate buffer pH 4.5 was fluxed on a single flow cell of the reactive matrix. In such a way, the NHS esters reacted spontaneously with the ligand amines to form covalent links. The injection of the ligand solution stopped when 110 resonance units (RU) of bound ligand were reached. Once the immobilization procedure was completed, non-specifically bound ligands were removed by washing with running buffer (50 mM PBS buffer pH 7.5 filtered with a 0.22 μM membrane filter, to which surfactant P20 0.005% from GE Healthcare was added) until the RU value became nearly constant. Reactive sites remaining on the surface were blocked by reaction with 1 M ethanolamine-HCl pH 8.5, fluxed over the two flow cells of the micro fluidic system with a flow rate of 10 μl/min for 7 min. Running buffer was again fluxed over the surface to stabilize the baseline. The reference flow cell was activated and deactivated without intermediate ligand immobilization in order to be used as a control surface for refractive index change and no specific binding during the kinetic analysis.

2.5. SPR binding experiment

Binding experiments were conducted by a kinetic titration method known as single-cycle kinetics (SCK) which consists in sequentially
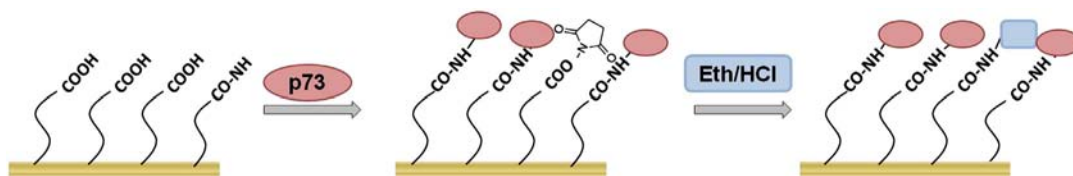
Fig. 3. Schematic representation of the covalent binding of the p73 protein on the SPR CM5 sensor chip. First, a mixture of EDC/NHS is injected over the chip to activate the surface, then p73 (pink ovals) is fluxed over the surface and the N-hydroxysuccinimide esters react spontaneously with its amino groups to form covalent links. Eventually, reactive sites remaining on the surface are blocked by reaction with 1 M ethanolamine-HCl (Eth/HCl) pH 8.5 (blue rectangles).

injecting increasing concentrations of the analyte over the functionalized sensor chip surface, without regeneration steps between each sample injection. It follows that the SCK method is faster than the classical one and that the ligand activity is fully preserved during the experiment, resulting in an increased efficiency and a reduction of costs.

To avoid excessive bulk effects, sensor chip surface was equilibrated with mutp53R175H protein buffer (Tris 100 mM, NaCl 300 mM DTT 1 mM buffer, pH 8) until the baseline was stable and then four increasing concentrations of mutp53R175H protein (analyte) in the range of 0.1–1.6 μM, serially diluted, were injected sequentially over both the ligand and the reference surfaces at a flow rate of 30 μl/min for 160 s. Also prior to the analyte binding cycle, buffer was injected for four binding cycles to have a blank response to be used for double reference (see Section 3.2). Analyte injections were followed by a 400 s dissociation step performed with a 30 μl/min flux of running buffer. Analytical cycles were programmed by means of a wizard template and the entire analysis was completely automated. To extract kinetic parameters from SPR data, systematic artifacts were removed using a two step data correction technique [36,37]. First, the response collected over the functionalized surface was subtracted by the response obtained from the reference one to remove bulk refractive index change, drift during association phase, jumps due to injection needle positioning. Second, the response from running buffer injection was subtracted. Sensorgrams were then globally fitted using BiaEvaluation software 2.1 (GE Healthcare, BIO-Sciences AB, Sweden) to a 1:1 interaction model [38] including the correction for mass transfer rate. Goodness of the fit was evaluated based on visual inspection, on the χ^2 value (expected to be lower than 10) and on the residual plots.

After substrate regeneration with a pulse of 10 mM NaOH solution, the interaction of p73 protein functionalized substrate with wtp53 protein was performed. The same experimental conditions (experimental method, analyte concentrations, flow rate, interaction and dissociation time) were set for the mutp53R175H/p73 protein interaction study in order to have comparable data.
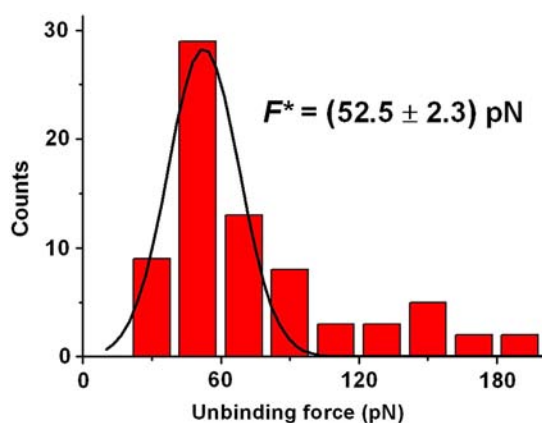
3. Results and discussion

3.1. AFS unbinding results

The histograms of the unbinding forces recorded at the different loading rates display similar shapes; a representative histogram corresponding to 1 nN s^{-1} loading rate being shown in Fig. 4.

However, the most probable unbinding force value (F^*) corresponding to the maximum of the main peak of each histogram, increases with the loading rate and shows values between 50 and 70 pN. These values fall in the range usually recorded for specific biological interactions [39]. The unbinding frequency, calculated as the ratio between the number of events corresponding to specific unbinding processes over the total recorded events, is about 11%. Such a value, which is somewhat lower than that expected for ligand–receptor pairs [25 and refs. therein], can be explained by considering that p73 is a big protein tightly packed on the glass substrate; this likely resulting into some steric hindrance which may limit the interaction with the partner. Additionally, the randomly bonded p73 protein via its lysine residues, may assume some orientations somewhat unfavorable to the complex formation.

According to the Bell–Evans model, the most probable unbinding force values F^* were plotted as a function of the natural logarithm of the loading rate (Fig. 5) in order to extract the kinetic parameters of the interaction. A single linear regime with ascending slope was observed and indicates the overcoming of a single barrier in the energy landscape. By fitting these data with Eq. (1), a width of the energy barrier $x_\beta = (1.32 \pm 0.28)$ nm and a dissociation rate constant, k_d, of $(1.18 \pm 0.07) \cdot 10^{-5}$ s^{-1} were found; both these values being typical of specific biological complexes [26].

According to the procedure described in detail elsewhere [40,41], the complex association rate constant (k_a) was also estimated, by using the expression $k_a = N_A \cdot V_{eff} / t_{0.5}$, where N_A is the Avogadro's number, V_{eff} is the effective volume of a half-sphere with radius r_{eff}

Fig. 4. Histogram of the unbinding forces for the mutp53R175H/p73 complex from AFS measurements carried out at a loading rate of 1 nN/s. The most probable unbinding force value, F^*, was determined from the maximum of the main peak of the histogram.
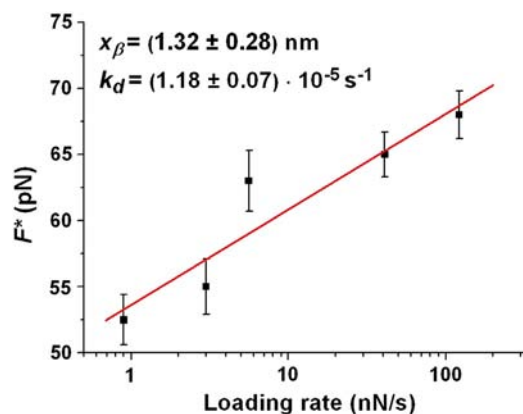

Fig. 5. The most probable unbinding force, F^*, plotted versus the logarithm of the loading rate r for the mutp53R175H/p73 complex, when p73 is immobilized on glass substrate and mutp53R175H is anchored on the AFS tip. The solid line is the bestfit of the experimental data by the Bell–Evans model (Eq. (1)); the extracted parameters k_d and x_β being reported.

around the tip, and $t_{0.5}$ is the time for the half-maximal binding probability given by $t_{0.5} = 2\, r_{eff}/v$, where v is the approach speed of the cantilever. A k_a of about 10^3 M^{-1} s^{-1} was thus found. The corresponding dissociation equilibrium constant ($K_D = k_d / k_a$) of the mutp53R175H/p73 complex was thus in the order of 10^{-8} M; this value positioning the complex in the 'affinity region' typical of antigen–antibody pairs which show a K_D in the range of 10^{-7}–10^{-11} M [26].

On the contrary, the AFS experiment carried out on the interaction between wild type 53 and p73 protein showed only a few number of unbinding specific events together with a negligible unbinding frequency (less than 3%). This is indicative that no significant interaction between p73 and wtp53 proteins is occurring. Such a result confirms previous data from the literature dealing with immunoprecipitation techniques of the whole cellular protein lysates [15].

3.2. SPR kinetic results

The SCK approach introduced by Karlsson and co workers [42] was used to study the interaction kinetics between mutp53R175H and p73 proteins. Fig. 6A (continuous line) shows the SPR signal (RU) as a function of time for successive injections of increasing concentrations of mutp53R175H. After the first injection with a 0.1 μM mutp53R175H solution, the signal increases nonlinearly approaching a plateau. Once the first injection is finished, the buffer is flowed over the ligand and the signal drops down, close to zero. The same trend is observed also for the successive injections of mutp53R175H. As far as higher mutp53R175H concentrations are used, progressively higher RU values are obtained; this being indicative of increasing levels of mutp53R175H (A, analyte) binding with the immobilized p73 (L, ligand). These kinetic data were analyzed in the framework of the Langmuir 1:1 binding model, which assumes a simple reversible bimolecular reaction between the ligand and the analyte [43,44] as described by the following equation:

$$A_{bulk} \underset{k_t}{\overset{k_t}{\rightleftarrows}} A_{surface} + L \underset{k_d}{\overset{k_a}{\rightleftarrows}} LA \qquad (2)$$

The model was modified to take into account the mass transport effect. In particular, the analyte is transferred from the bulk solution (A_{bulk}) towards the sensor chip surface, and $vice\ versa$, with a mass transfer coefficient, k_t, which is assumed to be the same in both directions. Then, the analyte that has reached the sensor chip surface ($A_{surface}$), binds to the ligand resulting in the formation of the ligand–analyte complex (LA) characterized by the association, k_a, and dissociation, k_d, rate constants. Accordingly, the variation of $A_{surface}$, L and LA concentrations with time, can be described by the following set of differential equations [45]:

$$\frac{d[A_{surface}]}{dt} = k_t\,([A_{bulk}] - [A_{surface}]) - (k_a[L][A_{surface}] - k_d[LA])$$
$$\frac{d[L]}{dt} = -(k_a[L][A_{surface}] - k_d[LA]) \qquad (3)$$
$$\frac{d[LA]}{dt} = (k_a[L][A_{surface}] - k_d[LA]).$$

To extract the kinetic parameters (k_a, k_d and K_D), the sensorgrams were globally fitted by a non linear least square analysis and numerical integration of Eq. (3) [46], by using the SPR evaluation software package. Such a fit, which is shown as dashed line in Fig. 6A, provided a k_a of $(6.4 \pm 0.5) \cdot 10^3$ M^{-1} s^{-1} and a k_d of $(3.1 \pm 1.8) \cdot 10^{-3}$ s^{-1}, with a χ^2 value of 2.24. These values resulted in a $K_D = k_d / k_a$ of $(4.9 \pm 0.6) \cdot 10^{-7}$ M.

The goodness of the 1:1 binding model was checked by generating the adsorption isotherm for the mutp73R175H/p73 system. The RU values reached at the steady state (R_{eq}) for each one of the sample injections shown in Fig. 6A were thus plotted $versus$ the corresponding concentrations of the mutp53R175H protein (Fig. 6B). Data were fitted (continuous line of Fig. 6B) by using Eq. (4), including a term for the bulk refractive index contribution (RI), which is assumed to be the same for all samples and which is used as the RU-axis offset:

$$R_{eq} = \frac{AR_{max}}{K_D + A} + RI \qquad (4)$$

where R_{max} is the analyte binding capacity of the surface and A is the analyte concentration. A K_D of $(8.0 \pm 2.2) \cdot 10^{-7}$ M, with a χ^2 value of 4.86, was obtained confirming the value provided by the global fitting procedures. Interestingly, it should be remarked that even if the two experimental approaches, AFS and SPR, operate at different conditions, they strongly support that mutp53R175H and p73 are engaged in the formation of a very specific complex which is characterized by a K_D typical of antigen–antibody pairs, what may be at the basis of the p73 sequestration and inactivation in cancerous cells. The one order of magnitude difference between the K_{Ds} provided by AFS and SPR, which are in the order of 10^{-7} M and 10^{-8} M, respectively, reflects essentially the difference in the dissociation rate constants, k_{ds}, obtained with the two methodologies. Such a difference should be attributed to the peculiarities of the two experimental techniques in which not only the interaction is monitored at level of single molecule in one case, AFS, and in bulk condition in the other, SPR, but also different substrates and
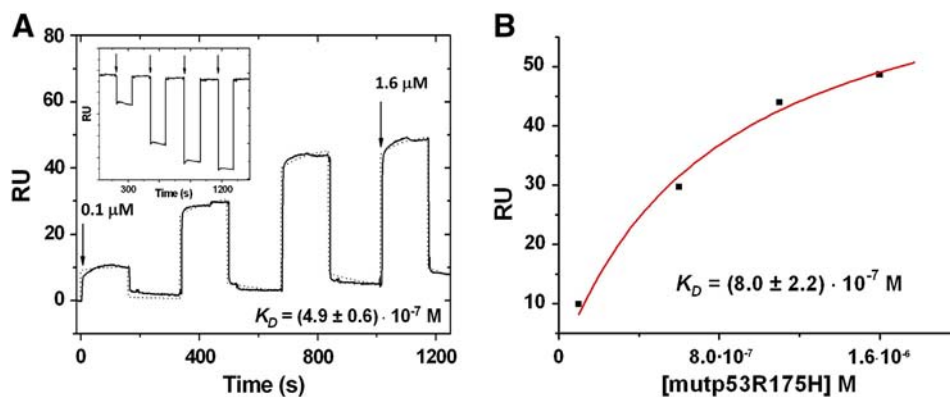

Fig. 6. SPR kinetic characterization of the interaction of mutp53R175H and wtp53 with p73 (A). Sensorgram of response curves (SPR signal in RU) versus time (solid line). Increasing concentrations of mutp53R175H protein solutions were injected sequentially over the substrate: 0.1 mM (1st arrow on the left), 0.6 mM (2nd injection), 1.1 mM (3rd injection) and 1.6 mM (4th injection, indicated with the arrow on the right). By fitting the sensorgram (dotted line) to a 1:1 binding model and taking into account the mass transport limitation, k_a, k_d and K_D values of the interaction are extrapolated. Inset: sensorgram of response curves versus time of increasingly concentrations of wtp53 injected over the p73 functionalized sensor chip surface. Arrows from left to the right indicate the successive injections of increasing concentrations of wtp53 over the substrate. No increase of the baseline signal is observed. (B) Binding affinity curve for the interaction of mutp53R175H protein onto p73 modified CM5 surface after titration with increasing concentrations of mutp53R175H protein. Equilibrium dissociation constant K_D was calculated by a fit through Eq. (4).

procedures are used to immobilize p73 protein on the substrate, what could lead to slight differences in the results [25].

The same procedure previously described for the SPR investigation of the interaction between mutp53R175H and p73, was used to investigate also the wtp53/p73 binding kinetics. In this case no increase of the SPR signal was observed after the injection of increasing wtp53 concentrations over the p73 functionalized sensor chip surface (see the inset of Fig. 6A). This is indicative of the lack of a specific interaction between wtp53 and p73 proteins. Again, both AFS and SPR experiments indicate that no interaction occurs between wtp53 and p73, confirming previous literature data obtained with immunoprecipitation techniques [15].

4. Conclusions

AFS and SPR have been used to investigate the interaction between p73 and both wild type p53 and the mutant p53R175H full length proteins in real time, in physiological conditions and without labels or sample manipulation. Both techniques confirm that conformational mutant mutp53R175H can physically interact with p73 resulting in the formation of a high affinity complex characterized by a K_D typical of antigen–antibody pairs, as well by a single well in the binding free energy. Additionally, AFS and SPR show that no interaction exists between wild type p53 and p73. The interaction between mutp53R175H and p73 deserves a high physiological relevance in cancer since the subsequent impairment of the p73 vicarious function of wtp53 would result in a marked chemoresistance of tumor cells [15,16,24]. Collectively, our results strongly suggest that the mutp53R175H/p73 complex could be a potential target for innovative pharmaceutical drugs. These indeed by binding to the mutp53R175H, could induce crucial conformational changes of the protein able to prevent its binding to p73 or could break the mutp53R175H/p73 complex restoring the p73 transcriptional and pro-apoptotic function. At least, the safeguard of the p73 antiproliferative activity may reduce the aggressiveness of cancerous cells carrying mutp53R175H protein and, at the same time, make them more responsive to common chemotherapeutic agents. It would be interesting to extend the present investigation approaches to study the interaction between p73 and other p53 mutants, also with the aim of screening suitable drugs able to inhibit the formation of the corresponding complexes.

Acknowledgements

References

[1] D.P. Lane, Cancer. p53, guardian of the genome, Nature 358 (1992) 15–16.
[2] C. Prives, P.A. Hall, The p53 pathway, J. Pathol. 187 (1999) 112–126.
[3] B. Vogelstein, D. Lane, A.J. Levine, Surfing the p53 network, Nature 408 (2000) 307–310.
[4] A.J. Levine, p53, the cellular gatekeeper for growth and division, Cell 88 (1997) 323–331.
[5] M.S. Greenblatt, W.P. Bennett, M. Hollstein, C.C. Harris, Mutations in the p53 tumor suppressor gene: clues to cancer etiology and molecular pathogenesis, Cancer Res. 54 (1994) 4855–4878.
[6] S. Di Agostino, S. Strano, V. Emiliozzi, V. Zerbini, M. Mottolese, A. Sacchi, G. Blandino, G. Piaggio, Gain of function of mutant p53: the mutant p53/NF-Y protein complex reveals an aberrant transcriptional mechanism of cell cycle regulation, Cancer Cell 10 (2006) 191–202.
[7] L. Weisz, A. Damalas, M. Liontos, P. Karakaidos, G. Fontemaggi, R. Maor-Aloni, M. Kalis, M. Levrero, S. Strano, V.G. Gorgoulis, V. Rotter, G. Blandino, M. Oren, Mutant p53 enhances nuclear factor kappaB activation by tumor necrosis factor alpha in cancer cells, Cancer Res. 67 (2007) 2396–2401.
[8] G. Fontemaggi, S. Dell'Orso, D. Trisciuoglio, T. Shay, E. Melucci, F. Fazi, I. Terrenato, M. Mottolese, P. Muti, E. Domany, D. Del Bufalo, S. Strano, G. Blandino, The execution of the transcriptional axis mutant p53, E2F1 and ID4 promotes tumor neo-angiogenesis, Nat. Struct. Mol. Biol. 16 (2009) 1086–1893.
[9] P. Stambolsky, Y. Tabach, G. Fontemaggi, L. Weisz, R. Maor-Aloni, Z. Siegfried, I. Shiff, I. Kogan, M. Shay, E. Kalo, G. Blandino, I. Simon, M. Oren, V. Rotter, Modulation of the vitamin D3 response by cancer-associated mutant p53, Cancer Cell 17 (2010) 273–285.
[10] M. Kaghad, H. Bonnet, A. Yang, L. Creancier, J.C. Biscan, A. Valent, A. Minty, P. Chalon, J.M. Lelias, X. Dumont, P. Ferrara, F. McKeon, D. Caput, Monoallelically expressed gene related to p53 at 1p36, a region frequently deleted in neuroblastoma and other human cancers, Cell 90 (1997) 809–819.
[11] H. Schmale, C. Bamberger, A novel protein with strong homology to the tumor suppressor p53, Oncogene 15 (1997) 1363–1367.
[12] C.A. Jost, M.C. Marin, W.G. Kaelin jr., p73 is a simian [correction of human] p53-related protein that can induce apoptosis, Nature 389 (1997) 191–194.
[13] W.G. Kaelin Jr., The p53 gene family, Oncogene 18 (1999) 7701–7705.
[14] L. Collavin, A. Lunardi, G. Del Sal, p53-family proteins and their regulators: hubs and spokes in tumor suppression, Cell Death Differ. 17 (2010) 901–911.
[15] C.J. Di Como, C. Gaiddon, C. Prives, p73 function is inhibited by tumor-derived p53 mutants in mammalian cells, Mol. Cell. Biol. 19 (1999) 1438–1449.
[16] S. Strano, E. Munarriz, M. Rossi, B. Cristofanelli, Y. Shaul, L. Castagnoli, A.J. Levine, A. Sacchi, G. Cesareni, M. Oren, G. Blandino, Physical and functional interaction between p53 mutants and different isoforms of p73, J. Biol. Chem. 275 (2000) 29503–29508.
[17] S. Strano, G. Fontemaggi, A. Costanzo, G. Rizzo, O. Monti, A. Baccarini, Physical interaction with human tumor derived p53 mutants inhibits p63 activities, J. Biol. Chem. 277 (2002) 18817–18826.
[18] E.R. Flores, S. Sengupta, J.B. Miller, J.J. Newman, R. Bronson, D. Crowley, A. Yang, F. McKeon, T. Jacks, Tumor predisposition in mice mutant for p63 and p73: evidence for broader tumor suppression functions for the p53 family, Cancer Cell 7 (2005) 363–373.
[19] A. Sigal, V. Rotter, Oncogenic mutations of the p53 tumor suppressor: the demons of the guardian of the genome, Cancer Res. 60 (2000) 6788–6793.
[20] S. Strano, S. Dell'Orso, S. Di Agostino, G. Fontemaggi, A. Sacchi, G. Blandino, Mutant p53: an oncogenic transcription factor, Oncogene 26 (2007) 2212–2219.
[21] M.S. Irwin, K. Kondo, M.C. Marin, L.S. Cheng, W.C. Hahn, W.G. Kaelin Jr., Chemosensitivity linked to p73 function, Cancer Cell 3 (2003) 403–410.
[22] D. Bergamaschi, M. Gasco, L. Hiller, A. Sullivan, N. Syed, G. Trigiante, I. Yulug, M. Merlano, G. Numico, A. Comino, M. Attard, O. Reelfs, B. Gusterson, A.K. Bell, V. Heath, M. Tavassoli, P.J. Farrell, P. Smith, X. Lu, T. Crook, p53 polymorphism influences response in cancer chemotherapy via modulation of p73-dependent apoptosis, Cancer Cell 3 (2003) 387–402.
[23] P. Lunghi, A. Costanzo, L. Mazzera, V. Rizzoli, M. Levrero, A. Bonati, The p53 family protein p73 provides new insights into cancer chemosensitivity and targeting, Clin. Cancer Res. 15 (2009) 6495–6502.
[24] S. Di Agostino, G. Cortese, O. Monti, S. Dell'Orso, A. Sacchi, M. Eisenstein, G. Citro, S. Strano, G. Blandino, The disruption of the protein complex mutantp53/p73 increases selectively the response of tumor cells to anticancer drugs, Cell Cycle 7 (2008) 3440–3447.
[25] A.R. Bizzarri, S. Cannistraro, Atomic force spectroscopy in biological complexes formation: strategies and perspectives, J. Phys. Chem. B 113 (2009) 16449–16464.
[26] A.R. Bizzarri, S. Cannistraro, The application of atomic force spectroscopy to the study of biological complexes undergoing a biorecognition process, Chem. Soc. Rev. 39 (2010) 734–749.
[27] J. Homola, S.S. Yee, G. Gauglitz, Surface plasmons resonance sensors: review, Sens. Actuators B 54 (1999) 3–15.
[28] M.A. Cooper, Label-free screening of bio-molecular interactions, Anal. Bioanal. Chem. 377 (2003) 834–842.
[29] A. Ebner, P. Hinterdorfer, H.J. Gruber, Comparison of different aminofunctionalization strategies for attachment of single antibodies to AFM cantilevers, Ultramicroscopy 107 (2007) 922–927.
[30] J.L. Hutter, J. Bechhoefer, Calibration of atomic-force microscope tips, Rev. Sci. Instrum. 64 (1993) 1868–1873.
[31] G.I. Bell, Models for the specific adhesion of cells to cells, Science 200 (1978) 618–627.
[32] R. Merkel, P. Nassoy, A. Leung, K. Ritchie, E. Evans, Energy landscapes of receptor–ligand bonds explored with dynamic force spectroscopy, Nature 397 (1999) 50–53.
[33] E. Evans, K. Ritchie, Dynamic strength of molecular adhesion bonds, Biophys. J. 72 (1997) 1541–1555.
[34] C. Friedsam, A.K. Wehle, F. Kuhner, H.E. Gaub, Dynamic single molecule force spectroscopy: bond rupture analysis with variable spacer length, J. Phys. Condens. Matter 13 (2003) S1709–S1723.
[35] B. Johnsson, S. Löfås, G. Lindquist, Immobilization of proteins to a carboxymethyldextran-modified gold surface for biospecific interaction analysis in surface plasmon resonance sensors, Anal. Biochem. 198 (1991) 268–277.
[36] D.G. Myszka, Improving biosensor analysis, J. Mol. Recognit. 12 (1999) 279–284.
[37] R.L. Rich, D.G. Myszka, Advances in surface plasmon resonance biosensor analysis, Curr. Opin. Biotechnol. 11 (2000) 54–61.
[38] T.A. Morton, D.G. Myszka, Kinetic analysis of macromolecular interaction using surface plasmon resonance biosensors, Methods Enzymol. 295 (1998) 268–294.
[39] J. Morfill, K. Blank, C. Zahnd, B. Luginbühl, F. Kühner, K.E. Gottschalk, K.E. Gottschalk, A. Plückthun, H.E. Gaub, Affinity-matured recombinant antibody fragments analyzed by single-molecule force spectroscopy, Biophys. J. 93 (2007) 3583–3590.
[40] A.R. Bizzarri, S. Santini, E. Coppari, M. Bucciantini, S. Di Agostino, T. Yamada, C.W. Beattie, S. Cannistraro, Interaction of an anticancer peptide fragment of azurin with p53 and its isolated domains studied by atomic force spectroscopy, Int. J. Nanomedicine 6 (2011) 3011–3019.

[41] M. Taranta, A.R. Bizzarri, S. Cannistraro, Probing the interaction between p53 and the bacterial protein azurin by single molecule force spectroscopy, J. Mol. Recognit. 21 (2008) 63–70.

[42] R. Karlsson, P.S. Katsamba, H. Nordin, E. Pol, D.G. Myszka, Analyzing a kinetic titration series using affinity biosensors, Anal. Biochem. 349 (2006) 136–147.

[43] P. Björquist, S. Boström, Determination of the kinetic constants of tissue factor/factor VII/factor VIIA and antithrombin/heparin using surface plasmon resonance, Thromb. Res. 85 (1997) 225–236.

[44] D.J. O'Shannessy, M. Brigham-Burke, K.K. Soneson, P. Hensley, I. Brooks, Determination of rate and equilibrium binding constants for macromolecular interactions using surface plasmon resonance: use of nonlinear least squares analysis methods, Anal. Biochem. 212 (1993) 457–468.

[45] R.W. Glaser, Antigen-antibody binding and mass transport by convection and diffusion to a surface: a two-dimensional computer model of binding and dissociation kinetics, Anal. Biochem. 213 (1993) 152–161.

[46] T.A. Morton, D.G. Myszka, I.M. Chaiken, Interpreting complex binding kinetics from optical biosensors: a comparison of analysis by linearization, the integrated rate equation, and numerical integration, Anal. Biochem. 227 (1995) 176–185.